Mathematical Modelling and Applications
2026, Vol. 11, No. 1, pp. 18–27
https://doi.org/10.11648/j.mma.20261101.12

SciencePG
Science Publishing Group

Research Article

Bifurcation and Stability Analysis of HIV-1 Coronavirus Co-infection Model

Cherono Pela[1, *], Kirui Wesley[2], Adicka Daniel[1]

[1]Department of Mathematics and Computer Science, University of Kabianga, Kericho, Kenya

[2]Department of Mathematics and Actuarial Science, South Eastern Kenya University, Kitui, Kenya

Abstract

The co-infection of HIV-1 viruses has emerged as a significant threat to global public health as a result of shared mode of transmission. This article presents a novel mathematical model that addresses the dynamics of this co-infection by extending the SVEIR (Susceptible – Vaccinated – Exposed – Infectious - Recovered) framework to incorporate time-delay, chemotherapy and quarantine compartments. The population is divided into twelve compartments, with infections individuals further subdivided into symptomatic and asymptomatic individuals. The mathematical model developed is constrained to adhere to fundamental epidemiology properties such as non-negativity and boundedness within a feasible. We investigate the fundamental reproduction number that guarantees stability of equilibrium points are disease free and endemic qualitative behavior of models are examined. Stability threshold explicitly state that when reproduction number is less than one the disease free equilibrium is globally asymptotically stable, meaning the infection can be eliminated. Using Lyapunov functions, local and global stability of these states are explored and findings presented graphically. They were used to account for the history dependent nature of time delay. Our research assessed control policies and proposed alternatives, performing bifurcation analysis so as to establish prevention strategies. We investigated Hopf bifurcation analytically and numerically to demonstrate disease dynamics, which is novel to our study.. Numerical simulations, performed using the MATLAB dde23 solver, demonstrate that the introduction of chemotherapy and quarantine significantly reduces the peak of symptomatic infections. Crucially, our Hopf bifurcation analysis identifies a critical delay threshold beyond which stable equilibrium is lost to sustained periodic oscillations, representing recurrent waves of infection or rather viral blips. This offered new insights into the long-term management of HIV-1 co-infection cycles.

Keywords

Coronavirus, Basic Reproduction Number, Global Stability, Lyapunov's Function, Bifurcation

1. Introduction

A disease called Coronavirus which had symptoms resembling that of pneumonia was reported in Wuhan China early December 2019. It was reported that it was the most devastating infectious disease caused by the novel Coronavirus SARS-CoV-2. It affected integration of communities worldwide in terms of health, economy and social interaction [22]. Due to weak immunity from other infections like HIV, pneumonia, tuberculosis and malaria, Coronavirus infection may be more

*Correspondence: Cherono Pela (pelacherono@gmail.com)

Received: 17 September 2025; **Accepted:** 21 January 2026; **Published:** 23 March 2026

common in people who already have such diseases. WHO implanted wearing of face mask, quarantine, vaccination, washing hands with alcohol as significant prevention and control strategies. Co-infection is when a single individual is infected by two or more pathogens or even different strains of the same pathogen. This is common in every society. Several scholars have investigated that Coronavirus disease infection is high in people living with other infections like cholera, tuberculosis and HIV who have compromised immunity. In order to understand the dynamics of infectious diseases mathematical modeling approaches have been used. Most scholars have formulated and analyzed mathematical models to investigate transmission dynamics of different infectious diseases using ordinary differential equations approach. [2, 9, 15, 17]. According to [6, 8, 12, 21] they developed and examined a co-infection model on HIV/AIDs and pneumonia by putting in control measures such as pneumonia vaccination and treatments of HIV/AIDs and pneumonia infections. They found out that pneumonia vaccination assisted in prevention of pneumonia infection. Similarly, [5, 3, 13, 17, 23, 27] costructed a mathematical model for Coronavirus and cholera co-infection that described the transmission dynamics of Coronavirus and cholera in Yemen. The model examined control measures such as lockdown, social distancing, number of test kits of control Coronavirus outbreak and number of susceptible individuals who can get CWTs for water purification. They found out that these four control measures played a major role in reducing the spread of Coronavirus. According to [4, 11, 15, 19, 22, 26] they developed a mathematical model on bifurcation and optimal control analysis of HIV-1 and Coronavirus co-infection with numerical simulation. They found out that backward bifurcation occurred whenever effective reproduction number is less than one. In their study, time-delay, vaccination and quarantine were not factored in. We therefore, suggest a delay nonlinear twelve-dimensional epidemic model to control the epidemic spread, vaccination and treatment of HIV-1 Coronavirus co-infection disease. Total population is denoted by $N(t)$. It is divided into 12-dimensional compartments.

2. Model Formulation

To explore transmission and control dynamics of co-infection between HIV-1 and Coronavirus, we partition total human population into twelve epidemiological compartments: susceptible individuals (S^*), vaccinated individuals (V^*), individuals not vaccinated (V_n^*), Exposed individuals (E^*), Exposed individuals with HIV-1 (E_h^*), Exposed individuals with AIDs (E_A^*), symptomatic individuals with AIDs (I_{sA}^*), symptomatic individuals with HIV-1 (I_{sh}^*), asymptomatic individuals with HIV-1 (I_{ah}^*), Quarantined individuals with HIV-1 (Q_h^*), Hospitalized individuals (H^*) and Removed individuals (R^*). Other parameters considered are:

Recruitment rate into susceptible class (ϕ_2), effective contact rate between S^* and V^* (β_3), effective contact rate between S^* and V_n^* (β_4), effective contact rate between V^* and E^* (α_3), effective contact rate between V_n^* and E^* (α_4), effective contact rate between V^* and R^* (α_5), effective contact rate between E^* and E_h^* (ω_3), effective contact rate between E^* and E_A^* (ω_4), effective contact rate between E_A^* and I_{sA}^* (ω_5), effective contact rate between E_h^* and I_{sh}^* (ω_6), effective contact rate between E_h^* and I_{ah}^* (ω_7), effective contact rate between H^* and R^* (γ_2), effective contact rate between I_{sh}^* and Q_h^* (γ_3), effective contact rate between I_{sA}^* and H^* (γ_4), effective contact rate between I_{ah}^* and $H^*(\gamma_5)$, effective contact rate between Q_h^* and R^* (δ_4), effective contact rate between Q_h^* and H^* (δ_5), Natural mortality rate (μ) and time-delay (τ). [11, 14, 18, 25].

2.1. Assumptions of the Model

The following are the model assumptions for this research work.

1) Dealing with closed population i.e no immigration nor emigration.
2) Mass action law applies.
3) Permanent immunity upon vaccination is attainable.
4) Removed class consists of individuals who recover naturally and through medication.
5) There is time lapse between exposure and being symptomatic.
6) A fraction of asymptomatic group goes to hospital on realizing that their contacts have been hospitalized or quarantined.
7) The rate of mortality is higher in infective cells followed by exposed cells, then recovered cells and lowest in susceptible cells i.e. $\mu_1 < \mu_4 < \mu_2 < \mu_3 \ldots < \mu_{16}$.

2.2. Mathematical Model

The dynamics of HIV-1 Coronavirus co-infection transmission system are governed by the following set of non-linear DDEs.

$$\frac{dS^*}{dt} = \emptyset_2 - \mu_5 S^* - \beta_2 S^* - \beta_3 S^*$$

$$\frac{dV^*}{dt} = \beta_2 S^* - \mu_6 V^* - \alpha_2 V_\tau^* - \alpha_4 V_\tau^*$$

$$\frac{dV_n^*}{dt} = \beta_3 S^* - \mu_7 V_\tau^* - \alpha_3 V_{n\tau}^*$$

$$\frac{dE^*}{dt} = \alpha_2 V_\tau^* + \alpha_3 V_{n\tau}^* - \mu_8 E^* - \omega_2 E_\tau^* - \omega_3 E_\tau^*$$

$$\frac{dE_A^*}{dt} = \omega_3 E_\tau^* - \mu_9 E_A^* - \omega_4 E_{A\tau}^*$$

$$\frac{dE_h^*}{dt} = \omega_2 E_\tau^* - \mu_{10} E_h^* - \omega_5 E_{h\tau}^* - \omega_6 E_{h\tau}^*$$

$$\frac{dI_{sh}^*}{dt} = \omega_5 E_{h\tau}^* - \mu_{11} I_{sh}^* - \gamma_1 I_{sh\tau}^*$$

$$\frac{dI_{ah}^*}{dt} = \omega_6 E_{h\tau}^* - \mu_{12} I_{ah}^* - \gamma_2 I_{ah\tau}^*$$

$$\frac{dI_{sA}^*}{dt} = \omega_4 E_{A\tau}^* - \mu_{13} I_{sA}^* - \gamma_3 I_{sA\tau}^*$$

$$\frac{dQ_h^*}{dt} = \gamma_1 I_{sh\tau}^* - \delta_1 Q_{h\tau}^* - \delta_2 Q_{h\tau}^* - \mu_{14} Q_h^*$$

$$\frac{dH_h^*}{dt} = \gamma_2 I_{sA\tau}^* + \gamma_3 I_{ah\tau}^* + \delta_2 Q_{h\tau}^* - \mu_{15} H_h^* - \Gamma_1 H_{h\tau}^*$$

$$\frac{dR^*}{dt} = \delta_1 Q_{h\tau}^* + \Gamma_1 H_{h\tau}^* + \alpha_4 V_{\tau}^*{}_{\tau} - \mu_{16} R^* \quad (1)$$

Subject to the following initial conditions:

$$S^*(0) \geq 0, V^*(0) \geq 0, V_n^*(0) \geq 0, E^*(0) \geq 0, E_A^*(0) \geq 0, E_h^*(0) \geq 0, I_{sh}^*(0) \geq 0, I_{ah}^*(0) \geq 0, I_{sA}^*(0) \geq 0, Q_h^*(0) \geq 0, H_h^*(0) \geq 0, R^*(0) \geq 0 \quad (2)$$

3. Theoretical Analysis

3.1. Positivity of Solutions

Theorem 3.1

Given non-negative initial conditions, all solutions of system (1) remain non-negative for all $t \geq 0$.

Proof: We prove non-negativity of every compartment in system (1) using contradiction and differential inequalities.

For $s^*(t) \geq 0$

Suppose there exist a first time $t_0 > 0$ such that $S^*(t_0) = 0$ with $S^*(t) > 0$ for $S^*(t_0) = 0$ with $S^*(t) > 0$ for $t < t_0$ and $S^*(t) < 0$ for $> t_0$. The governing equation is

$$\frac{dS^*}{dt} = \emptyset_2 - \mu_5 S^* - \beta_2 S^* - \beta_3 S^* \quad (3)$$

At $t = t_0$, since $S^*(t_0) = 0$ we have:

$$\frac{dS^*}{dt}_{t_0} = \emptyset_2 \geq 0 \quad (4)$$

which contradicts $S^*(t) < 0$ for $t < t_0$. Thus, $S^*(t) \geq 0$ for all $t \geq 0$.

Similarly, it can be shown that

$$(V^* > 0, V_n^* > 0, E^* > 0, E_A^* > 0, E_h^* > 0, I_{sh}^* > 0, I_{ah}^* > 0, I_{sA}^* > 0, Q_h^* > 0, H_h^* > 0, R^* > 0) \quad (5)$$

Hence, all compartments remain non-negative for all $t \geq 0$.

3.2. Model Analysis and Boundedness

Let's define;

$$N(t) = S^*(t) + V^*(t) + V_n^*(t) + E^*(t) + E_A^*(t) + E_h^*(t) + I_{sh}^*(t) + I_{ah}^*(t) + I_{sA}^*(t) + Q_h^*(t) + H_h^*(t) + R^*(t) \quad (6)$$

$$(dN(t))/dt = (d(S\hat{}*(t) + V\hat{}*(t) \llbracket + V \rrbracket\_n\hat{}*(t) + E\hat{}*(t) + E\_A\hat{}*(t) + E\_h\hat{}*(t) + I\_sh\hat{}*(t) \llbracket (t) + I \rrbracket\_ah\hat{}*(t) \llbracket (t) + I \rrbracket\_sA\hat{}*(t) + Q\_h\hat{}*(t) + H\_h\hat{}*(t) + R\hat{}*(t)))/dt \quad (7)$$

Thus,

$$\frac{dN(t)}{dt} \leq \emptyset_2 - \sum\mu. \text{ Where } \sum\mu = \mu_1 + \mu_2 + \cdots + \mu_{12}. \quad (8)$$

This implies that $N(t)$ is bounded and so

$$(S^*(t), V^*(t), V_n^*(t), E^*(t), E_A^*(t), E_h^*(t), I_{sh}^*(t), I_{ah}^*(t), I_{sA}^*(t), Q_h^*(t), H_h^*(t), R^*(t))$$

3.3. Basic Reproductive Number R_0 and Stability Analysis

The disease free equilibrium is the state of variable of the model in the absence of disease. Its stability can be tested using the eigenvalues of Jacobian matrix obtained at DFE, where at this point reproduction number is less than one. The linearization matrix of system (1) is given by:

$$\begin{bmatrix}
-\mu_5-\beta_2-\beta_3 & 0 & 0 & 0 & 0 & 0 & 0 & 0 & 0 & 0 & 0 & 0\\
\beta_2 & -\mu_6-\alpha_2e^{-\lambda\tau}-\alpha_4e^{-\lambda\tau} & 0 & 0 & 0 & 0 & 0 & 0 & 0 & 0 & 0 & 0\\
\beta_3 & 0 & -\mu_7-\alpha_3e^{-\lambda\tau} & 0 & 0 & 0 & 0 & 0 & 0 & 0 & 0 & 0\\
0 & \alpha_2e^{-\lambda\tau} & \alpha_3e^{-\lambda\tau} & -\mu_8-\omega_2e^{-\lambda\tau}-\omega_3e^{-\lambda\tau} & 0 & 0 & 0 & 0 & 0 & 0 & 0 & 0\\
0 & 0 & 0 & \omega_3e^{-\lambda\tau} & -\mu_9-\omega_4e^{-\lambda\tau} & 0 & 0 & 0 & 0 & 0 & 0 & 0\\
0 & 0 & 0 & \omega_2e^{-\lambda\tau} & 0 & -\mu_{10}-\omega_5e^{-\lambda\tau}-\omega_6e^{-\lambda\tau} & 0 & 0 & 0 & 0 & 0 & 0\\
0 & 0 & 0 & 0 & 0 & \omega_5\ e^{-\lambda\tau} & -\mu_{11}-\gamma_1e^{-\lambda\tau} & 0 & 0 & 0 & 0 & 0\\
0 & 0 & 0 & 0 & 0 & \omega_6e^{-\lambda\tau} & 0 & -\mu_{12}-\gamma_2e^{-\lambda\tau} & 0 & 0 & 0 & 0\\
0 & 0 & 0 & 0 & \omega_4e^{-\lambda\tau} & 0 & 0 & 0 & -\mu_{13}-\gamma_3e^{-\lambda\tau} & 0 & 0 & 0\\
0 & 0 & 0 & 0 & 0 & 0 & \gamma_1e^{-\lambda\tau} & 0 & 0 & -\delta_1e^{-\lambda\tau}-\delta_2e^{-\lambda\tau}-\mu_{14} & 0 & 0\\
0 & 0 & 0 & 0 & 0 & 0 & 0 & \gamma_3e^{-\lambda\tau} & \gamma_2e^{-\lambda\tau} & \delta_2e^{-\lambda\tau} & -\mu_{15} & -\Gamma_1e^{-\lambda\tau}\\
0 & 0 & \alpha_4e^{-\lambda\tau} & 0 & 0 & 0 & 0 & 0 & 0 & \delta_1e^{-\lambda\tau} & \Gamma_1e^{-\lambda\tau} & -\mu_{16}
\end{bmatrix}$$

The system (1) is locally asymptotically stable if all the eigenvalues of linearization matrix of system (1) (*) are negative. Clearly, the dominant eigenvalues is:

$$\lambda = -\mu_{14} + ((\delta_1 + \delta_2)e^{-\lambda\tau})$$

Theorem 1

Disease free equilibrium is stable whenever $R_0 < 1$ otherwise unstable.

Proof

λ_{10}^{**} should be negative. This can only be negative if;

$$\delta_1 e^{-\lambda\tau} < \delta_2 e^{-\lambda\tau} - \mu_{14}$$

Clearly,

$$\frac{\delta_1 e^{-\lambda\tau}}{\delta_2 e^{-\lambda\tau} - \mu_{14}} < 1 \tag{9}$$

Therefore $R_0 < 1$ is attained for DFE to be stable. [16, 20, 24].

3.4. Stability of Endemic Equilibrium Point

If all the eigenvalues of the linearization matrix about EEP are negative, then the system (1) is said to be stable. For stability analysis the equilibrium points are transformed to the origin.

We start by centering the model system (1) at endemic equilibrium $E(S^*, V^*, V_n^*, E^*, E_A^*, E_h^*, I_{sh}^*, I_{ah}^*, I_{sA}^*, Q_h^*, H^*, R^*)$ by introducing new variables $I_{ah}^*, I_{sA}^*, Q_h^*, H^*, R^*$

$$K_1 = S - S^*, K_2 = V - V^*, K_3 = V_n - V_n^*, K_4 = E - E^*, K_5 = E_A - E_A^*, K_6 = E_h - E_h^*, K_7 = I_{sh} - I_{sh}^*,\ K_8 = I_{ah} - I_{ah}^*, K_9 = I_{sA} - I_{sA}^*, K_{10} = Q_h - Q_h^* K_{11} = H - H^*,\ K_{12} = R - R^* \tag{10}$$

We then rewrite the model system (1) in terms of the new variables, and because $E(S^*, V^*, V_n^*, E^*, E_A^*, E_h^*, I_{sh}^*, I_{ah}^*, I_{sA}^*, Q_h^*, H^*, R^*)$ is an equilibrium point, the constant term cancel. We also discard the quadratic terms because their partial derivatives at the origin are zero.

The system (1) with the new variables becomes:

$$\dot{K}_1 = \emptyset_2 - (\mu_{5+}\beta_2 + \beta_3)(K_1 + S^*)$$

$$\dot{K}_2 = \beta_2(K_1 + S^*) - \mu_6(K_2 + V^*) - (\alpha_2 + \alpha_4)(K_{2\tau} + V_\tau^*)$$

$$\dot{K}_3 = \beta_3(K_1 + S^*) - \mu_7(K_3 + V_n^*) - \alpha_3(K_{3\tau} + V_{n\tau}^*)$$

$$\dot{K}_4 = \alpha_2(K_{2\tau} + V_{n\tau}^*) + \alpha_3(K_{3\tau} + V_{n\tau}^*) - \mu_8(K_4 + E^*) - (\omega_2 + \omega_3)(K_{4\tau} + E_\tau^*)$$

$$\dot{K}_5 = \omega_3(K_{4\tau} + E_\tau^*) - \mu_9(K_5 + E_A^*) - \omega_4(K_{5\tau} + E_{A\tau}^*))$$

$$\dot{K}_6 = \omega_2(K_{4\tau} + E_\tau^*) - \mu_{10}(K_6 + E_h^*) - (\omega_5 + \omega_6)(K_{6\tau} + E_{h\tau}^*)$$

$$\dot{K}_7 = \omega_5(K_{6\tau} + E_{h\tau}^*) - \mu_{11}(K_7 + I_{sh}^*) - \gamma_1(K_{7\tau} + I_{h\tau}^*)$$

$$\dot{K}_8 = \omega_6(K_{6\tau} + E_{h\tau}^*) - \mu_{12}(K_8 + I_{ah}^*) - \gamma_2(K_{8\tau} + I_{ah\tau}^*)$$

$$\dot{K}_9 = \omega_4(K_{5\tau} + E_{A\tau}^*) - \mu_{13}(K_9 + I_{sA}^*) - \gamma_3(K_{9\tau} + I_{sA\tau}^*)$$

$$\dot{K}_{10} = \gamma_1(K_{7\tau} + I_{sh\tau}^*) - (\partial_1 + \partial_2)(K_{10\tau} + Q_{h\tau}^*) - \mu_{14}(K_{10\tau} + Q_h^*)$$

$$\dot{K}_{11} = \gamma_2(K_{9\tau} + I_{sA\tau}^*) + \gamma_3(K_{8\tau} + I_{ah\tau}^*) + \partial_2(K_{10\tau} + Q_{h\tau}^*) - \mu_{15}(K_{11} + H^*) - \Gamma_1(K_{11\tau} + H_\tau^*)$$

$$\dot{K}_{12} = \partial_1(K_{10\tau} + Q_{h\tau}^*) + \Gamma_1(K_{11\tau} + H_\tau^*) + \alpha_4(K_{2\tau} + V_\tau^*) - \mu_{16}(K_{12} + R^*)$$

A solution of the form $K(t) = K_o e^{-\lambda t}$ and system (2) is linearized about the equilibrium

$$(K_1, K_2, K_3, K_4, K_5, K_6, K_7, K_8, K_9, K_{10}, K_{11}, K_{12}) = (S^*, V^*, V_n^*, E^*, E_A^*, E_h^*, I_{sh}^*, I_{ah}^*, I_{sA}^*, Q_h^*, H^*, R^*) \quad (11)$$

to obtain;

$$\dot{\hat{K}}(t) = B\hat{K}(t) \quad (12)$$

Differentiating system (2) partially with respect to state variables we obtain 12*12 matrix J_2;

$$\begin{bmatrix}
-\mu_5-\beta_2-\beta_3 & 0 & 0 & 0 & 0 & 0 & 0 & 0 & 0 & 0 & 0 & 0 \\
\beta_2 & -\mu_6-\alpha_2e^{-\lambda\tau}-\alpha_4e^{-\lambda\tau} & 0 & 0 & 0 & 0 & 0 & 0 & 0 & 0 & 0 & 0 \\
\beta_3 & 0 & -\mu_7-\alpha_3e^{-\lambda\tau} & 0 & 0 & 0 & 0 & 0 & 0 & 0 & 0 & 0 \\
0 & \alpha_2e^{-\lambda\tau} & \alpha_3e^{-\lambda\tau} & -\mu_8-\omega_2e^{-\lambda\tau}-\omega_3e^{-\lambda\tau} & 0 & 0 & 0 & 0 & 0 & 0 & 0 & 0 \\
0 & 0 & 0 & \omega_3e^{-\lambda\tau} & -\mu_9-\omega_4e^{-\lambda\tau} & 0 & 0 & 0 & 0 & 0 & 0 & 0 \\
0 & 0 & 0 & \omega_2e^{-\lambda\tau} & 0 & -\mu_{10}-\omega_5e^{-\lambda\tau}-\omega_6e^{-\lambda\tau} & 0 & 0 & 0 & 0 & 0 & 0 \\
0 & 0 & 0 & 0 & 0 & \omega_5\ e^{-\lambda\tau} & -\mu_{11}-\gamma_1e^{-\lambda\tau} & 0 & 0 & 0 & 0 & 0 \\
0 & 0 & 0 & 0 & 0 & \omega_6e^{-\lambda\tau} & 0 & -\mu_{12}-\gamma_2e^{-\lambda\tau} & 0 & 0 & 0 & 0 \\
0 & 0 & 0 & 0 & \omega_4e^{-\lambda\tau} & 0 & 0 & 0 & -\mu_{13}-\gamma_3e^{-\lambda\tau} & 0 & 0 & 0 \\
0 & 0 & 0 & 0 & 0 & 0 & \gamma_1e^{-\lambda\tau} & 0 & 0 & -(\delta_1+\delta_2)e^{-\lambda\tau}-\mu_{14} & 0 & 0 \\
0 & 0 & 0 & 0 & 0 & 0 & 0 & \gamma_3e^{-\lambda\tau} & \gamma_2e^{-\lambda\tau} & \delta_2e^{-\lambda\tau} & -\mu_{15}-\Gamma_1e^{-\lambda\tau} & 0 \\
0 & \alpha_4e^{-\lambda\tau} & 0 & 0 & 0 & 0 & 0 & 0 & 0 & \delta_1e^{-\lambda\tau} & \Gamma_1e^{-\lambda\tau} & -\mu_{16}
\end{bmatrix} \quad (13)$$

The system (2) is locally asymptotically stable if all the eigenvalues of linearization matrix of system (2) are negative. Clearly, the eigenvalues are:

$$\lambda_1^{***} = -(\mu_5 + \beta_2 + \beta_3)$$

$$\lambda_2^{***} = -(\mu_6 + (\alpha_2 + \alpha_4)e^{-\lambda\tau})$$

$$\lambda_3^{***} = -\mu_7 - \alpha_3 e^{-\lambda\tau}$$

$$\lambda_4^{***} = -(\mu_8 + (\omega_2 + \omega_3)e^{-\lambda\tau})$$

$$\lambda_5^{***} = -\mu_9 - \omega_4 e^{-\lambda\tau}$$

$$\lambda_6^{***} = -(\mu_{10} + (\omega_5 + \omega_6)e^{-\lambda\tau})$$

$$\lambda_7^{***} = -\mu_{11} - \gamma_1 e^{-\lambda\tau}$$

$$\lambda_8^{***} = -\mu_{12} - \gamma_2 e^{-\lambda\tau}$$

$$\lambda_9^{***} = -\mu_{13} - \gamma_3 e^{-\lambda\tau}$$

$$\lambda_{10}^{***} = -\mu_{16}$$

For λ_{11}^{***} and λ_{12}^{***} they are obtained from the characteristic equation below:

$$[(-\mu_{14} + ((\delta_1 + \delta_2)e^{-\lambda\tau})) - \lambda][(-\mu_{15} - \Gamma_1 e^{-\lambda\tau}) - \lambda] = 0 \quad (14)$$

$$\lambda^2 + a\lambda + b = 0 \quad (15)$$

$$\lambda_{11}^{***} = \frac{-a-\sqrt{a^2-4b}}{2}$$

$$\lambda_{12}^{***} = \frac{-a+\sqrt{a^2-4b}}{2}$$

Where,

$$a = \mu_{14} + \mu_{15} + \Gamma_1 e^{-\lambda\tau} + (\delta_1 + \delta_2)e^{-\lambda\tau}$$

$$b = \mu_{15}(\delta_1 + \delta_2)e^{-\lambda\tau} - \Gamma_1 e^{-2\lambda\tau}(\delta_1 + \delta_2) + \Gamma_1 e^{-\lambda\tau}$$

Therefore, Reproduction number at EEP is given by;

$$R_1 = \lambda_{12}^{***} = \frac{-a+\sqrt{a^2-4b}}{2}$$

Clearly,

$$R_1 = \frac{a^2}{a^2-4b} > 1 \quad (16)$$

The reproduction number at EEP is greater than one meaning that the disease existence persists hence becomes endemic.

3.5. Global Stability of Endemic Equilibrium

In this sub-section global stability of endemic equilibrium point ε^* is proofed by constructing Lyapunov functions.

Theorem 2

For system (1) endemic equilibrium is asymptotically stable when $R_0 > 1$ and otherwise unstable when $R_0 < 1$.

Proof

Consider the following Lyapunov function;

$\nu: \{((S^*, V^*, V_n^*, E^*, E_A^*, E_h^*, I_{sh}^*, I_{ah}^*, I_{sA}^*, Q_h^*, H^*, R^*) \in \Omega: (S^*, V^*, V_n^*, E^*, E_A^*, E_h^*, I_{sh}^*, I_{ah}^*, I_{sA}^*, Q_h^*, H^*, R^* > 0\} \to \mathbb{R}$ is given by

$$\nu((S^*, V^*, V_n^*, E^*, E_A^*, E_h^*, I_{sh}^*, I_{ah}^*, I_{sA}^*, Q_h^*, H^*, R^*) = \frac{1}{2}[(S^* - S^{**})^2 + (V^* - V^{**})^2 + \cdots + (R^* - R^{**})^2] \quad (17)$$

Differentiating ν with respect to t, we get,

$$\dot{v}((S^*, V^*, V_n^*, E^*, E_A^*, E_h^*, I_{sh}^*, I_{ah}^*, I_{sA}^*, Q_h^*, H^*, R^*) = (S^* - S^{**})\dot{S^*} + (V^* - V^{**})\dot{V^*} + \cdots (\dot{R^*} - R^{**})\dot{R^*} \quad (18)$$

$$= \left(1 - \frac{S^{**}}{S^*}\right)\dot{S} + \left(1 - \frac{V^{**}}{V^*}\right)\dot{V^*} + \cdots + (1 - \frac{R^{**}}{R^*})\dot{R^*} \quad (19)$$

$$= \left(1 - \frac{S^{**}}{S^*}\right)(\emptyset_2 - \mu_5 S^* - \beta_2 S^* - \beta_3 S^*) + \left(1 - \frac{V^{**}}{V^*}\right)(\beta_2 S^* - \mu_6 V^* - \alpha_2 V_\tau^* - \alpha_4 V_\tau^*) + \cdots + (1 - \frac{R^{**}}{R^*})(\delta_1 Q_{h\tau}^* + \Gamma_1 H_\tau^* + \alpha_4 V_\tau^* \ - \mu_{16} R^*) \quad (20)$$

By considering the system (1) (**) at endemic equilibrium point we have;

$$\emptyset_2 = \mu_5 S^{**} + \beta_2 S^{**} + \beta_3 S^{**}$$

$$\beta_2 S^{**} = \mu_6 V^{**} + \alpha_2 V_\tau^* + \alpha_4 V_\tau^*$$

$$\beta_3 S^{**} = \mu_7 V_{n\tau}^{**} + \alpha_3 V_{n\tau}^*$$

$$\alpha_2 V_\tau^{**} = -\alpha_3 V_{n\tau}^* + \mu_8 E^* + \omega_2 E_\tau^{**} + \omega_3 E_\tau^*$$

$$\omega_3 E_\tau^{**} = \mu_9 E_A^* + \omega_4 E_{A\tau}^*$$

$$\omega_2 E_\tau^{**} = \mu_{10} E_h^* + \omega_5 E_{h\tau}^{**} + \omega_6 E_{h\tau}^* \quad (21)$$

$$\omega_5 E_{h\tau}^{**} = \mu_{11} I_{sh} + \gamma_1 I_{sh\tau}^{**}$$

$$\omega_6 E_{h\tau}^{**} = \mu_{12} I_{ah}^* \mp I_{ah\tau}^*$$

$$\omega_4 E_{A\tau}^{**} = \mu_{13} I_{sA}^* + \gamma_3 I_{sA\tau}^*$$

$$\gamma_1 I_{sh\tau}^{**} = Q_{h\tau}^* + \delta_2 Q_{h\tau}^{**} + \mu_{14} Q_h^*$$

$$\gamma_2 I_{sA\tau}^{**} = -\gamma_3 I_{ah\tau}^* - \delta_2 Q_{h\tau}^{**} + \mu_{15} H^* + \Gamma_1 H_\tau^*$$

$$\delta_1 Q_{h\tau}^{**} = -\Gamma_1 H_\tau^* - \alpha_4 V_\tau^* + \mu_{16} R^*$$

Substituting the values obtained in equations (21) into equation (20) and simplifying we have;

$$\left(1 - \frac{S^{**}}{S^*}\right)(\emptyset_2 - \mu_5 S^* - \beta_2 S^* - \beta_3 S^*) + \left(1 - \frac{V^{**}}{V^*}\right)(\beta_2 S^* - \mu_6 V^* - \alpha_2 V_\tau^* - \alpha_4 V_\tau^*) + \cdots + (1 - \frac{R^{**}}{R^*})(\delta_1 Q_{h\tau}^* + \Gamma_1 H_\tau^* + \alpha_4 V_\tau^* \ - \mu_{16} R^*) \quad (22)$$

Here $v = 0$ when $(S^*, V^*, V_n^*, E^*, E_A^*, E_h^*, I_{sh}^*, I_{ah}^*, I_{sA}^*, Q_h^*, H^*, R^* = (S^{**}, V^{**}, V_n^{**}, E^{**}, E_A^{**}, E_h^{**}, I_{sh}^{**}, I_{ah}^{**}, I_{sA}^{**}, Q_h^{**}, H^{**}, R^{**})$. Otherwise $\dot{v} > 0$. Therefore the greatest compact invariant set in $\{(S^*, V^*, V_n^*, E^*, E_A^*, E_h^*, I_{sh}^*, I_{ah}^*, I_{sA}^*, Q_h^*, H^*, R^*) \in \Omega: \dot{v} > 0\}$ is the singleton $\{\varepsilon^*\}$, where ε^* is the endemic equilibrium point. It then implies that ε^* is globally asymptotically stable in the interior of Ω.

3.6. Birfucation Analysis

This section highlights the sufficient and necessary conditions for hopf bifurcation to occur using the bifurcating parameter time-delay τ. In this, we assume that $R_0 > 0$, that is, the endemic equilibrium ε^*, exists. To study stability of ε^*, we consider the linearization of the system (1) (*) at point ε^*.

Stability of EEP in absence of time-delay ($\tau = 0$).

From characteristic equation, clearly;

$$\lambda_{11}^{***} = \frac{-a - \sqrt{a^2 - 4b}}{2}$$

$$\lambda_{12}^{***} = \frac{-a + \sqrt{a^2 - 4b}}{2}$$

Where,

$$a = \mu_{14} + \mu_{15} + \Gamma_1 e^{-\lambda\tau} + (\delta_1 + \delta_2)e^{-\lambda\tau}$$

$$b = \mu_{15}(\delta_1 + \delta_2)e^{-\lambda\tau} - \Gamma_1 e^{-2\lambda\tau}(\delta_1 + \delta_2) + \Gamma_1 e^{-\lambda\tau}$$

Considering this when $\tau = 0$ then $\lambda_{11,12}^{***} < 0$ hence stability is guaranteed. This implies that in absence of delay i.e $\tau = 0$ and for $R_0 > 1$, the EEP is stable. This equilibrium creates people with co-nifections of HIV-1 Coronavirus disease.

Stability of EEP in presence of time-delay τ_i

In presence of time-delay τ_i, the eigenvalues obtained from the transcedendal equation that gave us the dominant eigenvalue at EEP compares to the one analyzed by Kirui *et al* (2015) and we use the same approach to find the roots of this equation analytically. Let $\lambda = x(\tau) + iy(\tau)$ be the eigenvalue of the characteristic equation. Since EEP is stable in absence of delay, it implies that $Re(\lambda) = x(0) < 0$. As τ increases from zero, there is a value $\tau_0 > 0$ such that EEP is stable for $\tau = [0, \tau_0]$ and unstable for $\tau > \tau_0$. At this threshold value, EEP loses stability and Hopf bifurcation occurs. Bifurcation value of $\tau_0 > 0$ occurs when $\lambda = x(\tau_0) + iy(\tau_0)$ is purely imaginary, that is $x(\tau_0) = 0$. This eigenvalue is defined as $\lambda = \pm iy_0$. Substituting this in the equation we obtain the following;

$$(iy_0)^2 + [a_1 + a_2 e^{-iy_0\tau}]iy_0 + a_3 e^{-iy_0\tau} - a_4 e^{-2iy_0\tau} \quad (23)$$

Where,

$$a_1 = \mu_{14} + \mu_{15}$$

$$a_2 = \Gamma_1 + \delta_1 + \delta_2$$

$$a_3 = (\mu_{15}(\delta_1 + \delta_2)$$

$$a_4 = (\delta_1 + \delta_2)\Gamma_1$$

Writing equation (10) in terms of trigonometric ratios,

$$-{y_0}^2 + ia_1y_0 + iy_0a_2[cosy_0\tau - isiny_0\tau] + a_3[cosy_0\tau - isiny_0\tau] - a_4[cos2y_0\tau - isin2y_0\tau] = 0 \quad (24)$$

Collecting real and imaginary we have that;

$$Im: -{y_0}^2 = y_0a_2siny\tau + a_3cosy_0\tau - a_4cos2y_0\tau \quad (25)$$

$$Re: a_1y_0 = y_0a_2cosy_0\tau - a_3siny_0\tau - a_4sin2y_0\tau \quad (26)$$

Adding the squares of both sides of equations (25) and (26) and collecting like terms one gets;

$${y_0}^4 + a_1^2{y_0}^2 = 0 \quad (27)$$

$$\text{Let } h(y_0) = {y_0}^4 + a_1^2{y_0}^2 \quad (28)$$

$$\text{Then } \frac{dh(y_0)}{dy_0} = 4{y_0}^3 + 2a_1^2y_0 > 0 \quad (29)$$

Since, $\frac{dh(y_0)}{dy_0}$ is positive it implies that λ crosses the imaginary axis with non-zero speed hence Hopf bifurcation occurs.

4. Main Results

Analytic solutions can be demonstrated using analytic results with specific numerical examples. The model system (1) (*) is considered. A numerical simulation of the model is calculated using list of parameters and their estimated values given in the Table 1. The values have been obtained from [1, 7, 10]. In simulation of the model system (1), the following initial values in each compartment at the onset of infection is assumed to apply;
$\left(S^*(0), V^*(0), V_n^*(0), E^*(0), E_A^*(0), E_h^*(0), I_{sh}^*(0), I_{ah}^*(0), I_{sA}^*(0), Q_h^*(0), H_h^*(0), R^*(0)\right) = (1000, 0, 0.01, 0.01, 500, 30, 0, 0, 0, 0, 0, 0)$ on the interval $[-\tau, 0]$.

Table 1. *The table of Variable, Variable description and Value.*

Parameters	Value	Source
S^*	2500	Fixed
V^*	1000	Estimated
V_n^*	1500	Estimated
E^*	100	Estimated
E_A^*	10	Estimated
E_h^*	10	Estimated
I_{sA}^*	0	Assumed
I_{sh}^*	0	Assumed
I_{ah}^*	0	Assumed
Q_h^*	15	Estimated
H^*	20	Estimated
R^*	5	Assumed
ϕ_2	2500	16
β_3	0.20	Assumed
β_4	0.002	14
α_3	0.53	Estimated
α_4	0.45	Estimated
α_5	0.50	Estimated

Parameters	Value	Source
ω_3	0.4	Estimated
ω_4	0.05	Estimated
ω_5	0.043	Estimated
ω_6	0.045	Estimated
ω_7	0.3425	Estimated
γ_2	0.05	22
γ_3	0.3	16
γ_4	0.3	16
γ_5	0.38	16
δ_4	0.200	22
δ_5	0.3	Assumed
μ	$0.019 < \mu < 0.51$	16

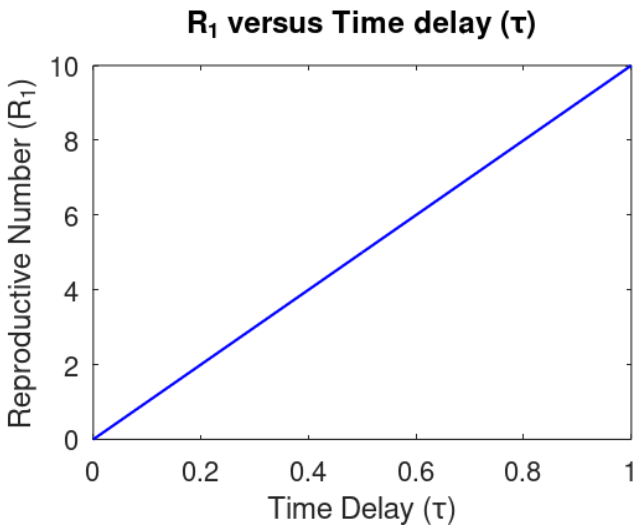

Figure 1. *A plot of R_1 against time against time-delay (τ).*

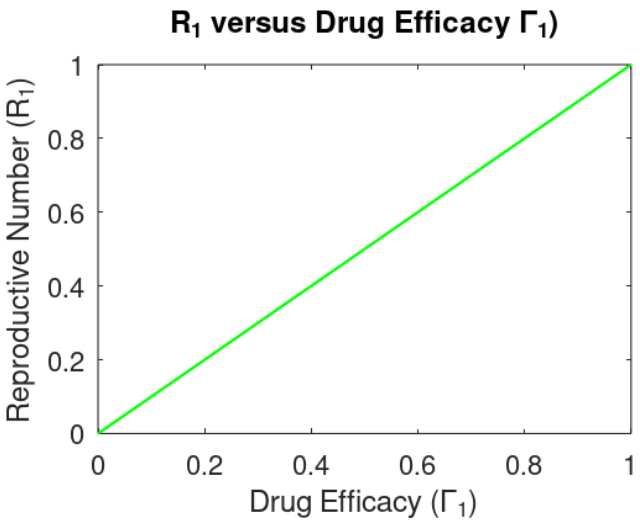

Figure 2. *A plot of R_1 against time against drug efficacy (Γ_1).*

Figure 1 shows a plot of reproduction number at EEP ($R1$) against the time-delay. It is evident that the time-delay affects the reproduction number at EEP. If this latent period is lengthened then stability is achieved.

Figure 2 shows a graph of Reproduction number at EEP against drug efficacy. It is evident that when drug efficacy is 100% the minimization of the growth of disease is achieved. At this point EEP is unstable.

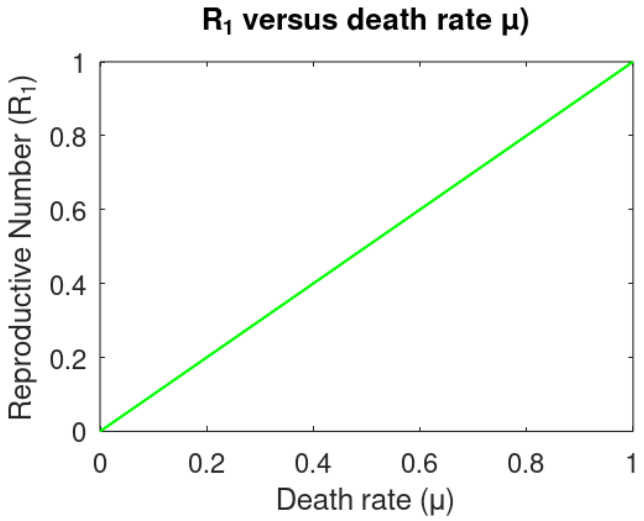

Figure 3. *A plot of R_1 against time against death rate (μ).*

Figure 3 shows a graph of reproduction number at EEP against death rate. It is evident from the graph that the higher the death rate the higher the reproduction number meaning that the disease is growing.

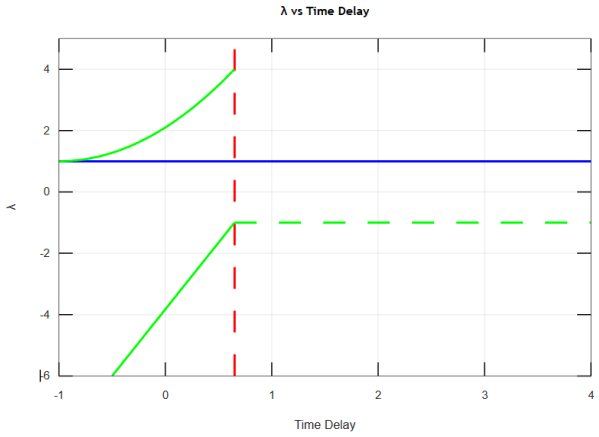

Figure 4. *A plot of λ against time-delay (τ).*

Figure 4 is a graph of lamda against time-delay. From the graph it is evident that the system (1) (*) is stable when time-delay is less than the threshold value of 0.56 days. Above this threshold value hopf bifurcation occurs that destabilizes the equilibrium.

5. Conclusion

In this study, a SVEIR model for HIV-1 and Coronavirus disease co-infection was developed. This model incorporates vaccination, quarantine, chemotherapy and time-delay to analyze the dynamics of the disease. To measure the spread of the disease, Basic Reproduction Number R_0 was used. Disease Free Equilibrium (DFE) is attained when $R_0 < 1$. This is affected by vaccination, time-delay, quarantine and chemotherapy of both HIV-1 and Coronavirus. The study found out that if all other factors are kept constant then DFE is achieved when drug efficacy is above 50%. From the numerical analysis it is clear that for time-delay $\tau > 0$ DFE is stable and unstable otherwise.

To understand the dynamics of the disease, local and global stabilities of the SVEIR model were determined using Lyapunov functions. It was found out that local stability is attained when $R_0 < 1$ and global stability is achieved when $R_0 > 1$. Finally, Bifurcation analysis was carried out to determine the effect of changing time-delay parameter τ on the equilibrium of the SVEIR model. It was found out that for the threshold value $\tau = 0.56$, the system is in equilibrium. When this value is changed, oscillation occurs. This causes instability resulting in the Hopf Bifurcation.

Abbreviations

DDE	Delay Differential Equations
DFE	Disease Free Equilibrium
EEP	Endemic Equilibrium Point
HIV	Human Immuno Deficiency Virus
J	Jacobian
WHO	World Health Organisation

Conflicts of Interest

The authors declare no conflicts of interest.

References

[1] Byul Nim, Eunjung Kim, Sunmi Lee, and Chunyoung Oh, 2020, Mathematical Model of COVID-19 Transmission Dynamics in South Korea The Impact of Tavel Restrictions, Social Distancing and Early Detection, Journal of Maths MDPI Publishers pg 1-18.

[2] Sarbaz H. A. Khoshnaw, Rizgar H. Salih and Sadegh Sulaimany, 2020, Mathematical Modelling for Coronavirus diseases (COVID-19) in Predicting future behaviours and sensitivity Analysis, Journal of Mathematical Modelling of Natural Phenomena.

[3] Anwar Zeb, Ebraheem Alzahrani, Vedat Suat Erturk and Gul Zaman, 2020, Journal of Biomed Research International Hindawi Publishers, volume 2020, 7 pages.

[4] Viona Ojiambo, Mark Kimathi, Samuel Mwalili, Duncan Gathungu, Rachel W. Mbogo, 2020, A Human-pathogen SEIR-P Model for COVID-19 Outbreak Under different intervention Scenario in Kenya, journal of Mathematics, pg 1-10.

[5] Pakwan Riyapan, Sherif Eneye Shualb and Arthit Intarasit. 2021. A Mathematical Model of COVID-19 Pandemic A case Study of Bangkok, Thailand, Journal of Computational and Mathematical methods in medicine, Hindawi Publishers, 11 pages.

[6] Betti, M.; Bragazzi N.; Heffernan, J.; Kong, J.; Raad, A. Could a New COVID-19 Mutant Strain Undermine Vaccination Efforts? A Mathematical modelling approach for estimating the spread of B.1.1.7 Using Ontario, Canada as a Case Study Vaccines, 2021, a, 592.

[7] Ali Alarjani, Md Taufiq Nasseef, Sanaa M. Sharif B. V. Subba Rao, Mufti Mahmud and Md Sharif Uddin, 2020, Application of Mathematical modelling in prediction of COVID-19 transmission dynamics, Journal of computer engineering and computer science, Springer open publishers.

[8] Rahim Ud Din, Kamal Shah, Imtiaz Ahmad and Thabet Abdelijawed, 2020, study of transmission dynamics of novel COVID-19 by using mathematical model, Journal of Advances in Difference Equations, Springer open publishers, pg 1-13.

[9] Liu, T.; Kang, L.; Li, Y.; Huang, J.; GUO, Z; Xu, J.; Hu, Y.; Zhai, Z.; Kang, X.; Jiang, T.; et al. Simultaneous Detection of seven Human Coronaviruses by multiplex PCR and MALDI-TOFMS. COVID 2022, 2, 5-17.
https.//doi.org/10.3390/covid2010002

[10] Elrashdy, F.; E. M.; Uversky, V. N. on the safety of covid-19 convalescent plasma treatment: Thrombotic and Thromboembolic concerns. COVID 2022, 2, 1-4.
https://doi.org/10.3390/covid2010001

[11] Hirota, K.; Mayahara, T.; Fujii, Y.; Nishi, K. Asymptomatic Hypoxemia as a characteristic symptom of coronavirus Disease. A narrative Review of its pathophysiology. COVID 2022, 2, 47-59.

[12] Chable-Bessia, C,; Boulle, C; Neyret, A.; Swain, J.; Henaut, M.; Merida, P.; Gros, N.; Makinson, A.; Lyonnais, S.; Chesnais, C.; et al. Low selectivity indices of invermectin and macrocyclic lactones on SARS-COV-2 Replication in vitro. COVID 2022, 60-75.

[13] Kaur, A.; Michalopous C.; Carpe, S; Congrete, S.; Shahzad, H,; Reardon, J.; Wakefield, D.; Swart, C.; Zuwallack, R. Post-covid-19 condition and health status 2022, 2, 76-86 (MDPI) Publishers.

[14] Peronace, C.; Tallerico, R.; Colosimo, M.; Panduri, G.; Pintomalli, L.; Oteri R.; Calantoni, V.; et al (2022) B A. I Omicron Variant of SARS-COV-2: First Case Reported in Calabria Region, Italy. COVID 2022, 2, 211-215.

[15] Schlickeiser, R.; Kroger, M. Forecast of Omicron Wave Time Evolution. COVID 2022, 2, 216-229.

[16] Cho, D-H.; Choi, J.; Gwon, J. G. Atorvastatin Reduces Severity of COVID-19: A Nationwide, Total population-Based, case-control study. COVID 2022, 2, 398-406.

[17] Sorensen, C. A.; Clemmensen, A.; Sparrewath, C.; Tetens, M. M.; Krogfelt, K. A. Children Naturally Evading COVID-19-Why Children Differ from Adults. COVID 2022, 2, 369-378.

[18] Batra, A.; Swaby, J.; Raval, P.; Zhu, H.; Weintraub, N. L.; Terris, M.; Karim, N. A.; Keruakous, A.; Gulterman, D.; Beyer, K.; et al. Effect of community and socio-economic factors on cardiovascular, cancer and cardio-oncology patients with COVID-19. COVID 2022, 2, 350-368.

[19] Mbhiza and Muthelo (2022) COVID-19 and the Quality of mathematics education, teaching and learning in a first-year course. South African Journal of Higher education volume 36 Number 2 pages 189-203.
https://dx.doi.org/10.20853/36-2-4676

[20] N. Ringa, M. L. Diagne, H. Rwezaura, A. Omame, S. Y. Tchoumi and J. M. Tchuenche (2022) HIV and COVID-19 co-infection: A mathematical model and optimal control. Journal of informatics medicine Elsevier publishers page 1-17
https//doi.org/10.1016/j.imu.2022.100978

[21] Kassahun Getnet Mekonen, Shiferaw Feyissa Balcha, Legesse Lemecha Obsu and Abdulkadir Hassen (2022) Mathematical modeling and Analysis of TB and COVID-19 Coinfection. Journal of applied mathematics Hindawi publishers pages 1-20.

[22] Kotola, B. S., Teklu, S. W., and Abebaw, Y. F. (2023). Bifurcation and optimal control analysis.

[23] Kirui W., R. K. (2015). Modelling the effects of time delay on HIV-1 in vivo dynamics in the presence of ARVs. *Science Journal of Applied Mathematics and Statistics*, 204-213.

[24] O. Diekmann, J. H. (1990). On the definition and computation of Ro in models for infectious diseases in heterogeneous populations. Journal of Mathematical Biology, 365-382.

[25] Watmough, P. D. (2002). Reproduction numbers and sub-threshold endemic equilibria for compartmental models of disease transmission. Journal of Mathematical Biosciences, 29-48.

[26] Lawrence Shampine and Skip Thompson (2000), Solving delay differential equations with dde23, Southern Methodist University and Radford University, pages 1-44.

[27] Hezam Ibrahim M., F. A. (2021). A dynamic optimal control model for COVID-19 and cholera co-infection in Yemen. Advances in Difference Equations.